Plant Physiology and Biochemistry 195 (2023) 182–192

Contents lists available at ScienceDirect

Plant Physiology and Biochemistry

journal homepage: www.elsevier.com/locate/plaphy

B" and C subunits of PP2A regulate the levels of reactive oxygen species and superoxide dismutase activities in Arabidopsis

Csongor Freytag [a], Tamás Garda [a], Zoltán Kónya [b], Márta M-Hamvas [a], Balázs Tóth-Várady [a], Gabriella Petra Juhász [a], László Ujlaky-Nagy [c], Adrienn Kelemen [a], Gábor Vasas [a], Csaba Máthé [a,*]

[a] Department of Botany, Faculty of Science and Technology, University of Debrecen, Hungary
[b] Department of Medical Chemisty, Faculty of Medicine, University of Debrecen, Hungary
[c] Department of Biophysics and Cell Biology, Faculty of Medicine, University of Debrecen, Hungary

ARTICLE INFO

Handling Editor: Dr K Kees Venema

Keywords:
Protein phosphatase PP2A
B" subunit
C3C4 subunits
Oxidative stress
Phosphorylated H2AX
Superoxide dismutase
Cu/Zn-SOD

ABSTRACT

The serine-threonine protein phosphatases PP2A regulate many cellular processes, however their role in oxidative stress responses and defence is less known. We show the involvement of its C (catalytic) and B" (a regulatory) subunits. The *c3c4* (C subunit) and *fass* (B") subunit mutants and Col wt of Arabidopsis were used. Controls and treatments with the PP2A inhibitor microcystin-LR (MCY-LR) and reactive oxygen species (ROS) inducer diquat (DQ) were employed. ROS levels of primary roots were largely genotype dependent and both C and B" subunit mutants had increased sensitivity to MCY-LR and DQ indicating the involvement of these subunits in oxidative stress induction. Superoxide dismutases (SOD), mainly the Cu/Zn-SOD isoform, as key enzymes involved in ROS scavenging are also showing altered (mostly increased) activities in both *c3c4* and *fass* mutants and have opposite relations to ROS induction. This indicates that the two types of subunits involved have partially different regulatory roles. In relation to this, control and MCY-LR/DQ treated B" subunit mutants were proven to have altered levels of phosphorylation of histone H2AX. γH2AX, the phosphorylated form indicates double stranded DNA damage during oxidative stress. Overall we point out the probable pivotal role of several PP2A subunits in the regulation of oxidative stress responses in plants and pave the way for future research to reveal the signaling pathways involved.

1. Introduction

Oxidative responses accompany normal developmental and physiological events (cell division, photosynthetic and mitochondrial electron transport etc.) and are induced by a variety of abiotic and biotic stresses in plants (Apel and Hirt, 2004). This involves elevations of reactive oxygen species (ROS) as well as changes of levels and activities of antioxidant enzymes (Apel and Hirt, 2004). Reversible protein phosphorylation is important in the regulation of many cellular events and oxidative stress signaling pathways often involve these post-translational modification mechanisms. Protein phosphatases that target phosphorylated side chains of serine and threonine amino acids are the main players in the relevant protein dephosphorylation (see Shi, 2009; Máthé et al., 2019 for reviews). ABI1 is a PP2C that belongs to the metal dependent protein phosphatases (Meinhard and Grill, 2001). It negatively regulates ABA signaling, increases ROS levels and keeps ROS scavenging enzyme activities at relatively low levels (Ludwików et al., 2014). This well-known fact points out the important role of well regulated protein dephosphorylation in plant ROS signaling. This raises the question whether the non-metal dependent PP2A, a serine-threonine phosphatase crucial in the regulation of intracellular processes (Shi, 2009) has such a role as well.

PP2A is a complex consisting of an "A" scaffolding, a "B" regulatory and a "C" catalytic subunit (Shi, 2009). Arabidopsis has five catalytic (C) subunits of PP2A (Farkas et al., 2007). Among them, C3 and C4 subunits belong to the subfamily II (Yoon et al., 2018). They are involved in (i) the organization of mitotic and non-mitotic microtubules; (ii) the regulation of PIN phosporylation and in consequence, auxin distribution

* Corresponding author. Egyetem ter 1, H-4032, Debrecen, Hungary.
E-mail addresses: freytagcsongor@gmail.com (C. Freytag), gtamas0516@gmail.com (T. Garda), konya.zoltan@med.unideb.hu (Z. Kónya), hamvas.marta@science.unideb.hu (M. M-Hamvas), tothvaradyb@gmail.com (B. Tóth-Várady), juhaszgabriellapetra@gmail.com (G.P. Juhász), lnagy@med.unideb.hu (L. Ujlaky-Nagy), keleadri0613@gmail.com (A. Kelemen), vasas.gabor@science.unideb.hu (G. Vasas), mathe.csaba@science.unideb.hu (C. Máthé).

https://doi.org/10.1016/j.plaphy.2022.12.031
Received 12 October 2022; Received in revised form 14 December 2022; Accepted 31 December 2022
Available online 31 December 2022

within embryos and roots which influence their developmental patterning; (iii) the light-dependent regulation of nitrate reductase (Ballesteros et al., 2013; Spinner et al., 2013; Creighton et al., 2017). The *c3c4* double mutant is characterized by severe impairment of root and shoot development and related to this, severely altered microtubule organization (Spinner et al., 2013). There is a high variety of "B" subunits grouped into subfamilies (B, B', B") that regulate not only the activity, but the subcellular localization of the holoenzymes as well (Farkas et al., 2007; Shi, 2009). Many functions of these subunits are known, but less knowledge for their involvement in ROS signaling is known to date. The *ton2/fass* mutants have disfunctional or absent PP2A/B" regulatory subunits and the homozygote recessive phenotypes are dwarf, practically lacking roots and the preprophase band of microtubules important in the organization of mitotic division plane is absent. B" subunits are known to interact with C3 and C4 (Camilleri et al., 2002; Spinner et al., 2013).

Superoxide dismutases (SODs) are main scavengers of ROS by dismutating the superoxide anion to form hydrogen-peroxide, a less toxic form of ROS (Kliebenstein et al., 1998). According to their metal dependence, there are multiple isoforms of SOD. Fe-SOD isoenzymes are localized mainly in chloroplasts, but they are also present in the cytosol and nucleus in plants including non-photosynthetizing organs. Concerning roots, most of Fe1-SOD is localized in the apical region, but present in the whole primary root system of young seedlings where it contributes to the development of salt stress tolerance (Dvořák et al., 2021). Mn-SOD is localized essentially in mitochondria and peroxisomes, but a putative apoplastic form was also identified in Arabidopsis roots (Chen et al., 2022). Cu/Zn SOD is localized mainly in the plastids and also present in the cytosol, peroxisomes and apoplast (Kliebenstein et al., 1998; Gill et al., 2015). In plants, not much is known on the dependence of their levels and/or activities on direct or indirect phosphoregulation.

H2AX is a variant of histone H2A in eukaryotes. Its phosphorylated form at the carboxy-terminal site is called γH2AX that marks DNA double-strand breaks induced e.g. by ROS and plays a role in the initiation of double-stranded DNA repair (Fillingham et al., 2006; Tanaka et al., 2006). This latter function is achieved by triggering nucleosome loss to allow recruitment of protein complexes important in repair (Fuchs et al., 2006). In plants, little is known on the role of phosphatases such as PP2A in the direct regulation of H2AX phosphorylation state (see Discussion as well).

We used Arabidopsis Columbia wild-type plants as well as *fass* and *c3c4* mutants throughout our experiments, as tools for the study of involvement of PP2A in ROS signaling. Both control and drug treated seedlings were employed. The two drugs (toxins) used were microcystin-LR (MCY-LR) and diquat (DQ). MCY-LR is a cyclic heptapeptide produced by several cyanobacterial strains known to be a potent inhibitor of the serine-treonine protein phosphatase PP2A (and PP1). For PP2A, it affects mainly the C subunit by its competitive binding to the active site of the enzyme (MacKintosh and MacKintosh, 1994; MacKintosh and Diplexcito, 2001). DQ, as paraquat (PQ) is a dihydropyridine herbicide that is inducing strong oxidative stress in plants including Arabidopsis (Lv et al., 2021). The toxicity of DQ is practically identical to PQ: it induces the transfer of electrons from PSI to O_2, thus creating ROS. Although for the above reason it affects mainly photosynthetic organs, it alters normal growth and development of roots as well (Acar, 2021; Lv et al., 2021). The background of this phenomenon is that DQ/PQ affect mitochondrial electron transport chain not only in animal, but in non-photosynthetic plant cells as well (Zer et al., 1993; Chen et al., 2021). Thus, DQ is not known to interfere with any protein phosphatases, making it ideal to be used as a comparative tool in this study.

In the light of the above statements, the principal aim of this work is to give novel insights in the role of several isoforms of PP2A subunits in plant oxidative stress. These are C3 and C4 for the catalytic and B" for the B regulatory subunits. All are well known to regulate important subcellular events (see Discussion section as well), but our knowledge related to their role in the regulation of ROS levels and/or scavenging is much less. In relation to the PP2A-ROS relationship, we intend to answer the following question as well: is the phosphorylation state of histone H2AX regulated by PP2A?

2. Materials and methods

2.1. Plant material and treatments

The genotypes of *Arabidopsis thaliana* used in this study were the wild-type Columbia as well as protein phosphatase (PP2A) related mutants described by Camilleri et al. (2002), Kirik et al. (2012) and Spinner et al. (2013). These were *c3c4*, a double mutant for the respective catalytic subunits and the *fass* (*ton2*) mutants for the B" regulatory subunit. The *fass-15* and *fass-5* mutants used here are created by similar methods (EMS mutagenesis), but the degree of Fass *same* protein modification is different. These latter mutants exhibit their abnormal phenotypes only when their genotypes are homozygote recessive. In the present study we used both homozygotes (HoZ) and heterozygotes (HeZ) the latter being in fact pools of seedlings consisting of the homozygote dominant genotype (in fact Col0) and HeZs. These pools are referred hereafter as HeZs. All mutants were a kind gift of Dr. Martine Pastuglia, Institut Jean-Pierre Bourgin, INRA Versailles, France.

Seed sterilization, seedling culture and the method for MCY-LR/DQ treatments were performed essentially according to Nagy et al. (2018) and Freytag et al. (2021). Briefly, seeds were sterilized with commercial bleach and washed thereafter, followed by their transfer to a modified Murashige-Skoog medium (Murashige and Skoog, 1962; Gamborg et al., 1968). After a 48 h-cold treatment, plates with seeds were transferred to a plant tissue culture chamber under a 14/10 h photoperiod, 22 ± 2 °C, 60 μmol $m^{-2}s^{-1}$ photon flux density in the light period. Five days after, seedlings were transferred on sterilized filter paper soaked in liquid modified MS media and MCY-LR/DQ treatments started. These treatments lasted for 24 h for each type of experiments presented in this study.

Microcystin-LR (MCY-LR) was purified in our laboratories by a method described by Kós et al. (1995) as modified by Vasas et al. (2004). Methanolic cyanobacterial (*Microcystis aeruginosa* BGSD243) extracts were subjected to ion-exchange, then size exclusion chromatography. Purity of preparations was checked by a HPLC method (see Freytag et al., 2021). Diquat dibromide monohydrate (DQ) was purchased from Supelco, Bellefonte, PA. Concentrations of MCY-LR and DQ used in this study were carefully chosen-for our purposes, non-lethal concentrations (at least for the 24h treatment period) were chosen which still induced oxidative stress responses.

For histochemistry and immunohistochemistry studies (determination of total ROS contents, immunohistochemical detection of γH2AX), we used primary roots for all the Arabidopsis genotypes involved. For the biochemical studies (Western blot detection of γH2AX and in-gel detection of SOD activities), we used primary roots for Col0 and the *fass* HeZs. For the *fass* HoZ and *c3c4*, since they barely developed well defined roots or the biomass of roots was very low, we used whole seedlings for these biochemical studies.

2.2. The assay of total reactive oxygen species (ROS) levels in roots

For the tissue localization and quantification of ROS, we used roots from living seedlings of all genotypes involved in this study. 2′,7′-dichlorofluorescein-diacetate (DCFH-DA) is a good method to assay intracellular total ROS in plants (Jambunathan, 2010). Accordingly, roots were washed in phosphate buffered saline (PBS), then directly stained with 10 μM DCFH-DA (Sigma-Aldrich, St. Louis, Mo). dissolved in PBS (pH 7.0) as described by Garda et al. (2016). To avoid the formation of photon-induced artefacts during DCFH-DA labeling, the entire procedure was performed in dark. Samples were excited at 450–480 nm and examined with a conventional Olympus BX43 fluorescence

microscope (Olympus, Tokyo, Japan). Fluorescence intensities (number of pixels showing area integrated optical density/AIOD) for primary root tips and differentiated root tissues were quantified with the Fiji software (Schindelin et al., 2012). Roots of at least five seedlings per treatment per experiment were used and five independent experiments were performed.

2.3. Detection and quantification of γH2AX in roots

Phosphorylated histone H2AX (γH2AX) was examined both by immunolocalization and Western blot.

The immunofluorescence procedure followed the principles of a whole mount protocol as described by Pasternak et al. (2015) and Freytag et al. (2021) with slight modifications. Briefly, intact tips of control and MCY-LR/DQ treated primary roots of Col0 were fixed with 2% (w/v) paraformaldehyde (PFA) + 0.1% (v/v) Triton-X100 in 2x microtubule stabilizing buffer (MTSB). Vacuum infiltration was used for 5 min twice, then further incubation occurred for 50 min without vacuum; then samples were washed with 1x MTSB three times. Root tips were then treated with methanol and rehydrated with a series of decreasing methanol concentrations. Afterwards, cell walls were digested with 2% (w/v) Driselase (Sigma-Aldrich, St. Louis, Mo., USA) and 0.2% macerozyme (Serva Electrophoresis GmbH, Heidelberg, Germany) in 2 mM MES (Sigma-Aldrich) for 30 min at 37 °C and samples were washed with 1x MTSB. Seedlings were then permeabilized with 10% (v/v) DMSO/3% (v/v) IGEPAL (Sigma-Aldrich) in 1x MTSB for 20 min at 37 °C and washed with 1x MTSB. Samples were pre-incubated in 1x MTSB +4% (w/v) BSA (Sigma-Aldrich) for 30 min and incubated with primary antibody in 1x MTSB + 4% BSA 4h at 37 °C (or overnight at 4 °C), then washed with 1x MTSB. The primary antibody was rabbit raised anti-γH2AX2 (Thermo Fisher Scientific, Waltham, USA PA5-77995) at a 1:30 dilution. Secondary antibody was Alexa 488 conjugated anti-rabbit IgG generated in goat (Abcam, Cambridge, UK). Incubation with secondary antibody was in 1x MTSB +4% BSA for 4h at 37 °C, then samples were washed with 1x MTSB. Preparations were analyzed with a Zeiss LSM 880 (Carl Zeiss AG, Jena, Germany) confocal microscope with Zen Black 2.3 software and the conventional settings for Alexa 488 visualization (Arg laser for excitation; emission was observed with the aid of a 490 nm dichroic mirror and a 490–530 filter set). Samples were then counterstained with 3 μg mL^{-1} 4′6′-diamidino-2-phenylindole (DAPI, Fluka, Buchs, Switzerland) to visualize all nuclei according to Beyer et al. (2012). DAPI visualization was performed with a 405 nm diode laser and signal detection was as for the conventional LSM parameters for this dye. Quantification of γH2AX labeling intensity was performed with the aid of the Fiji software (Linkert et al., 2010; Schindelin et al., 2012) and given as number of pixels showing area integrated optical density/AIOD. Roots of at least five seedlings per treatment per experiment were used and five independent experiments were performed.

Western blot studies designed for the quantification of γH2AX were performed according to the method of Waadt et al. (2008) as modified in our laboratory and involved control and MCY-LR/DQ treated whole roots or whole seedlings (the type of plant material depended on the genotype as described at Section 2.1.) of all genotypes involved in this study. To summarize, whole roots or seedlings were homogenized, then boiled at 95 °C for 5 min in a buffer containing 50 mM Tris pH 8.0; 150 mM NaCl; 1%SDS, 1 mM phenyl methyl sulphonyl fluoride (PMSF, PanReac AppliChem, Darmstadt, Germany), 1x protease inhibitor cocktail (Sigma-Aldrich), 4% poly-vinyl-pyrrolidone (PVP). Extracts were then centrifuged at 13,000 rpm for 20 min (Beckman Avanti series centrifuge, Indianapolis, USA) at 10–15 °C. Protein content of supernatants was assayed with a BCA reagent, then Laemmli buffer was added and samples were subjected to boiling at 95 °C for 3 min. Equal amounts of proteins (30 μg) were loaded on gels, along with a molecular weight marker (Thermo Fisher Scientific). Running gel contained 15% (w/v) polyacrylamide. SDS-PAGE was according to Laemmli (1970). Proteins were blotted into nitrocellulose membranes (Millipore, Burlington, Ma., USA) with an electroblot system (Cleaver Scientific, Rugby, UK). The transfer buffer was 25 mM Tris; 192 mM glycine; 20% (v/v) methanol; pH 8.3. Membranes were then blocked with 1xTBST (1xTBS + 0,05% Tween 20) + 3% (w/v) BSA for 2 h at room temperature. Afterwards, primary antibodies were applied. Anti – γH2AX from rabbit (Thermo Fisher Scientific) was used at a dilution (in TBST + 3% BSA) of 1:3000, while anti – β – tubulin (Abcam) was used as a loading control at a dilution of 1:12,000. Labeling was performed overnight at 4 °C. After several washing steps, a HRP conjugated anti-rabbit secondary antibody (Abcam) was applied at a 1:4000 dilution for 2 h at room temperature. After several washing steps, protein bands were detected by the Chemidoc chemoluminescence system (BioRad, Hercules, USA). For the Western blot studies, roots of at least thirty seedlings or a similar number of whole seedlings per treatment per experiment were used and three independent experiments were performed.

2.4. In-gel detection of superoxide dismutase (SOD) isoenzyme activities - roots and whole plants

The in-gel assay of SOD activities was an adaptation of the methods described by Giannopolitis and Ries (1977) and Bertrand and Eze (2014). Plant material was ground in liquid nitrogen, then extracted in a buffer containing phosphate buffer, pH 7.5, 4% (w/v) PVP, 1x protease inhibitor cocktail, (Sigma-Aldrich), 1 mM PMSF (PanReac, Applichem, USA). Extracts were centrifuged as for the Western-blot analysis (see section 2.3.), then protein content of samples was measured according to Bradford (1976). Equal amounts of proteins (40 μg) were loaded into each well of gels, samples contained Laemmli buffer without SDS. The running gel contained 10% polyacrylamide without SDS. Following separation of proteins, gels were washed with sterile water, then incubated in 2.5 mM nitroblue tetrazolium (NBT, Duchefa, Haarlem, The Netherlands) for 20 min, followed by incubation in 28 μM riboflavin +28 μM N, N, N ′, N′-tetramethyl-ethylene-diamine (TEMED, Sigma-Aldrich). Gels were illuminated (1050 lumen LED light source) to reveal bright SOD activity bands in a dark background. Band intensities correlated with enzyme activities and were quantified with the GelAnalyzer 19.1® software (www.gelanalyzer.com, by Istvan Lazar Jr., PhD and Istvan Lazar Sr., PhD, CSc). For the in-gel SOD activity assays, roots of at least thirty seedlings (or the corresponding number of whole seedlings) per treatment per experiment were used and three independent experiments were performed.

2.5. Data analysis

All quantified data were plotted –plots are showing the mean ± SE values-with the aid of Systat Sigma Plot 10.0 ® software (Systat Software, San Jose, CA). Statistical significances for the differences between groups controls and treatments were studied by two-way ANOVA (post-hoc: Holm-Sidak method) and t-tests (the latter only for Fig. 2 where only one variable is analyzed). Differences were considered to be significant at $P < 0.1$ according to the statistical settings used. During data analysis we took into consideration the hypothesis of alterations of the studied parameters by MCY-LR and DQ and that separate two factors were analyzed (dependence on genotype and MCY-LR/DQ treatments). P values are marked in figures by 3 levels: treatments within genotype (against control), P value < 0,001 ***; <0,05 **; <0,1 *; changes in control (not MCY-LR/DQ treated) mutants as compared to Col0, P value: <0,001 × × ×; <0,05 × ×; <0,1 ×. As stated in the above sections, for every experiment we used minimum 3 independent observations per group. In the case of SOD activity assays and Western blot analyses, approximately 30 seedlings were in groups, furthermore we scrutinized at least five seedlings per group during microscopic examination.

3. Results

3.1. Protein phosphatase mutants of Arabidopsis have altered ROS levels and MCY-LR/DQ treatments increase their sensitivity to oxidative stress

When we compared primary roots of control genotypes (i.e. no MCY-LR/DQ treatments) of Arabidopsis Columbia wild-type to protein phosphatase mutants, we detected marked differences in terms of ROS levels. The *c3c4* (catalytic subunit) mutants showed similar ROS levels in the tips of primary roots, but significantly lower levels in differentiated primary root tissues (Fig. 1b, d). In contrast, homozygote recessive genotypes of *fass-5* and *fass-15* (B" subunit) showed significant differences to Col0 in root tips (Fig. 1b, arrows). *fass-5*, where the homozygote recessive (HoZ) genotype shows more severe phenotypic alteration than *fass-15* (Spinner et al., 2013), has higher levels of ROS than Col0 and even *fass-15*, and this is true for both the homozygote recessive and the HeZ genotypes (Fig. 1a–c, arrows). For *fass-5*, differentiated roots could be examined only for the HeZs (Fig. 1c), since the HoZ did not develop well differentiated root tissues.

The reactions to drugs of primary roots from different genotypes did differ as well. Col0 roots did not show significant changes of ROS contents at MCY-LR/DQ treatments (Fig. 1a–d). In contrast, *c3c4* mutants were characterized by significantly elevated levels of total ROS at treatments with both the PP2A inhibitor MCY-LR and the ROS inducer DQ, in the tips of primary roots (Fig. 1b, d). In the differentiation zone both MCY-LR and DQ induced ROS elevation as well, but these elevated *c3c4* ROS values are still below the levels of ROS levels in Col0 controls (Fig. 1d). For the *fass-15* mutants, in case of HeZs MCY-LR and DQ treatments induced only slight increases in root tips and DQ induced significant elevations of ROS levels in differentiated root tissues (Fig. 1a, c). For the HoZ recessives, 1 μM MCY-LR and 1 μM DQ increases ROS levels in differentiated root tissues in a significant manner (Fig. 1b, d). For the *fass-5* mutant, 1 μM MCY-LR had a significantly increasing effect in root tips of HoZs (Fig. 1b). 0.5 μM DQ increased, while 1 μM DQ decreased significantly ROS levels both in HoZs and HeZs in all root developmental zones where they could be examined (Fig. 1a–c).

3.2. MCY-LR and DQ alter γH2AX levels in a genotype dependent manner

Immunohistochemical labeling of Col0 primary root tips for γH2AX showed that nearly all nuclei contained this post-translational modification (Fig. 2a) and MCY-LR altered slightly its levels (Fig. 2 c). In contrast, DQ induced a significant and strong increase in the phosphorylation level of H2AX (Fig. 2b and c).

At a comparison of different genotype controls, a thorough Western blot analysis of whole seedling protein extracts proved marked differences for the *fass-15* and *fass-5* homozygotes that showed higher γH2AX levels, than *Col0* and *c3c4* (Fig. 3a/lower panel, 3d, arrows). In the case of roots of *fass* HeZs, we could not detect such increases in *fass*, as compared to Col0 (Fig. 3a, upper panel; Fig. 3b). As for drug treatments, MCY-LR increased the amount of phosphorylated H2AX in Col0 and *fass-5*/HeZ roots (Fig. 3a/upper panel, 3c, arrow). Interestingly for extracts of whole seedlings of *fass-5* homozygotes, both MCY-LR and DQ treatments decreased and not increased γH2AX levels (Fig. 3e, arrows). Neither MCY-LR, nor DQ induced marked changes in *c3c4* and *fass-15* (Fig. 3a, lower panel; 3c, e).

3.3. Activities of superoxide dismutase (SOD) isoenzymes change in a genotype and MCY-LR/DQ treatment dependent manner

Native activity gels for SOD showed three distinct groups of SOD activities. Inhibition studies with KCN and H_2O_2 revealed the location of Mn-SOD, Fe-SOD and Cu/Zn SOD activity bands (data not shown). The most prominent activity bands were detected for Mn-SOD and Fe-SOD (Fig. 4e).

At an examination of protein extracts from whole seedlings, Mn-SOD activities were similar for Col0 vs. HoZ recessives of *fass-15* and *fass-5* as well as *c3c4* and MCY-LR/DQ treatments did not change this activity in a significant manner (Fig. 4a and b). Fe-SOD activities were higher in controls of *fass-15* and *c3c4* as compared to Col0 controls (Fig. 4a, arrow). Neither MCY-LR, nor DQ had any significant effects on Fe-SOD activities for any of the genotypes, except a slight decrease in *fass-5* in the presence of 0.5 μM DQ (Fig. 4c). The most prominent changes could

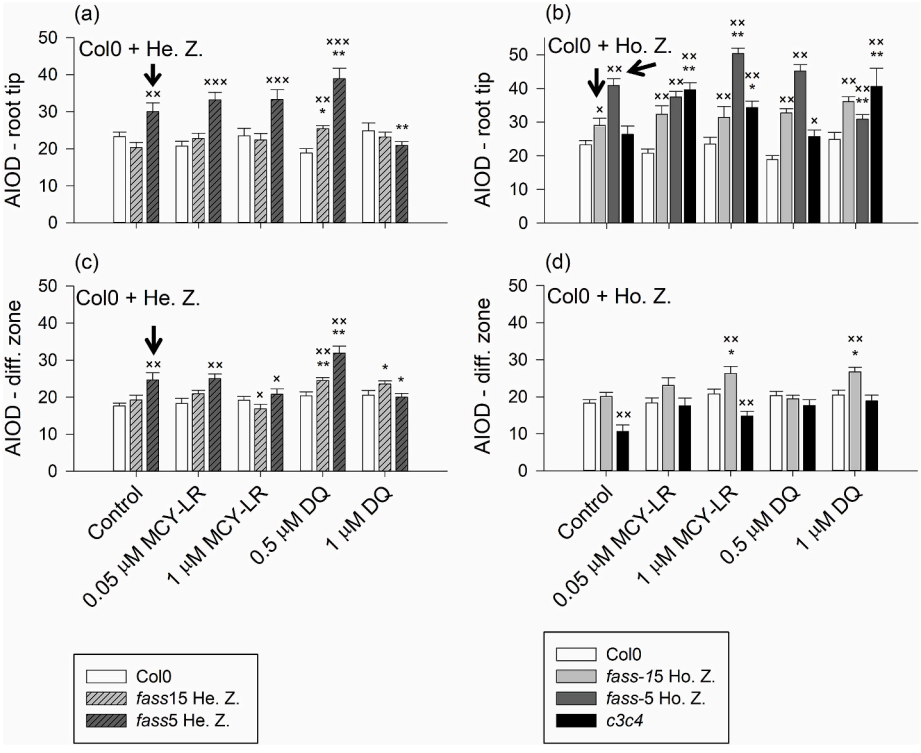

Fig. 1. Total ROS contents of wild-type and phosphatase mutant primary roots in root tips (**a, b**) and differentiated root tissues (**c, d**) as revealed by DCFH-DA staining. Both controls and toxin (MCY-LR and DQ) treatments are shown. These data reveal that ROS contents differ significantly in a genotype and toxin treatment dependent manner. (**a, c**) Col wt vs. *fass* (B" subunit) mutant heterozygotes; (**b, d**) Col wt vs. *fass* (B" subunit mutant), homozygote recessives and *c3c4* (catalytic subunit mutant) homozygote recessives. Arrows on (a, b, c) indicate that in controls of *fass* mutants, ROS levels are higher, than in Col0 controls. Significant differences ($P < 0.1$) are indicated by * and ** (significance of differences between controls and treatments within a given genotype) and "X, XX and XXX" (significant differences as compared to Col0 controls) according to Section 2.5. of Materials and methods.

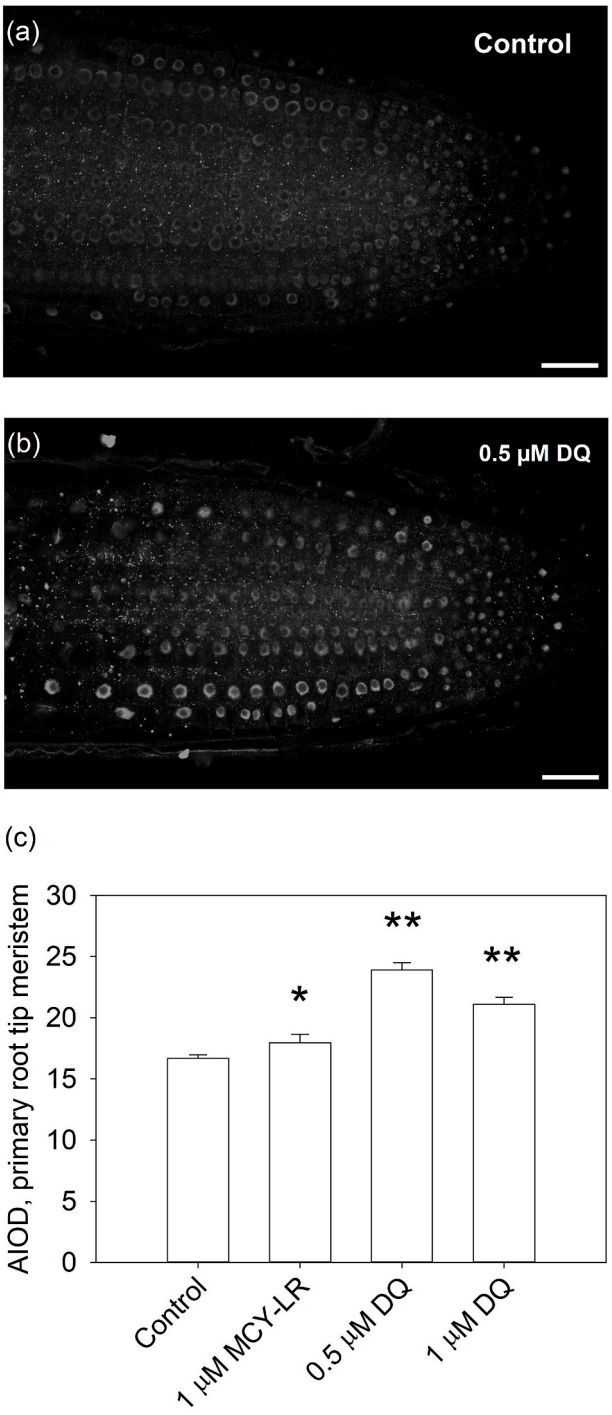

Fig. 2. Immunohistochemical labeling reveals that DQ and less, MCY-LR increase the levels of γH2AX in tips of Col wt roots. (a, b) Representative confocal microscopy images of single stacks of control (**a**) and 0.5 μM DQ treated (**b**) samples labeled with anti- γH2AX. Scalebars: 25 μm. (**c**) quantification of results (labeling intensities) at MCY-LR and DQ treatments. Significant differences ($P < 0.1$) are indicated by * and ** (significance of differences between controls and treatments) according to Section 2.5. of Materials and methods.

be observed for Cu/Zn SOD activities. Control *fass* and *c3c4* seedlings had significantly higher activities, than Col0 (Fig. 4a, arrows). Both MCY-LR and 0.5 μM DQ increased Cu/Zn-SOD activities in Col0 and *fass* – but not in *c3c4* -, with the most significant/prominent changes in *fass-5* (Fig. 4d, arrows). In this latter case, a high concentration (1 μM) of DQ decreased the activity (Fig. 4d).

Root extracts of Col0 plants as well as HeZs of *fass-15* and *fass-5* were examined for SOD activities as well. As seen for the experiments with whole seedlings (see above), no genotype- or MCY-LR/DQ-dependent changes were observed for Mn-SOD activities (Fig. 5a and b). In contrast, Fe-SOD activities were significantly lower in controls of *fass-15* as compared to the other two genotypes (Fig. 5a, arrow). MCY-LR and DQ treatments induced slight, but non-significant increases in Col0, *fass-5* and *c3c4* (Fig. 5c). For *fass-15*, only DQ induced such changes (Fig. 5c). Cu/Zn-SOD activities were similar in all three genotypes (controls, Fig. 5a) and MCY-LR/DQ treatments induced visible, but non-significant increases in Col0 and *fass* mutants, with the most prominent changes in MCY-LR treated *fass-5* (Fig. 5d/see arrows). These effects were partially similar to those observed for whole plants of Col0 and HZ recessives of *fass* (Fig. 4d).

4. Discussion

Overexpression of PP1 (a non-metal dependent phosphatase), for which the catalytic subunit is related to PP2A/C, induces increased non-enzymatic ROS scavenging capacity, APX activity and reduced malondialdehyde content under salt stress in rice. These results suggest that PP1 is involved in the regulation of oxidative stress responses in this plant (Liao et al., 2016). PP2A is the most frequent among serine-threonine phosphatases in plants, but its relationship to oxidative stress regulation is much less known in plants. However, there are some data regarding especially the B' regulatory subunits, as we will show below.

The B'γ subunit of PP2A activates PP2A holoenzyme in the absence of biotic stresses (Li et al., 2014). During pathogenesis response (PR), this subunit is inactivated which will increase the phosphorylation state of CONSTITUTIVE EXPRESSION OF PR GENES5 (CPR5), a factor involved in ROS signaling: it will activate the respiratory burst oxidase homologue (RBOH) and increase the expression of an ascorbate peroxidase isoform (APX2) (Trotta et al., 2011b; Li et al., 2014; Konert et al., 2015). The Arabidopsis *pp2a-b'γ* mutants are characterized by increased levels of Cu/Zn SOD in leaves (Trotta et al., 2011a, b). The B'θ subunit localizes PP2A to the peroxisomes, where it has an activating effect. Upon pathogen attack it is inactivated to trigger PR (Kataya et al., 2015).

Fass mutants affect a putative B" subunit of PP2A (Camilleri et al., 2002; Spinner et al., 2013). As stated in the Introduction section, this subunit is involved in key developmental processes like regulation of mitotic microtubular organization. However, B" subunit, a principal target of this study was not shown yet unequivocally to regulate ROS signaling.

The C3 and C4 catalytic subunits of PP2A are regulating cortical microtubule organization during salt stress (Yoon et al., 2018). Since C4 subunit is involved in SnRK mediated ABA signaling (Waadt et al., 2015; Máthé et al., 2019) that is regulating ROS generation-related gene expression, it is likely that it can trigger oxidative stress. However, to date there was no evidence on the direct involvement of C3 and C4 in plant oxidative stress. Thus, the present study is one of the first ones to demonstrate this relationship. In the light of the above statements, the present work intends to give an essential contribution to this issue as regarding the C3–C4 catalytic and B" regulatory subunits of PP2A.

4.1. B" and C3/C4 subunits of PP2A regulate ROS levels and their scavenging by SOD

The present study shows that the roots of *c3c4* double loss-of function mutant of Arabidopsis are characterized by lower ROS levels than wild-type roots, but concerning oxidative stress, by higher sensitivity to the PP2A inhibitor MCY-LR and the ROS inducer DQ (Fig. 1b, d). This is accompanied by higher capacity of ROS scavenging by Fe1-SOD and Cu/Zn-SOD for *c3c4* controls. However, MCY-LR treatments do not modify further these SOD activities, thus we can state here that there is no direct relationship between ROS levels and scavenging in MCY-LR treated *c3c4* (Fig. 1b, d; 4). In contrast, the controls of homozygote recessive

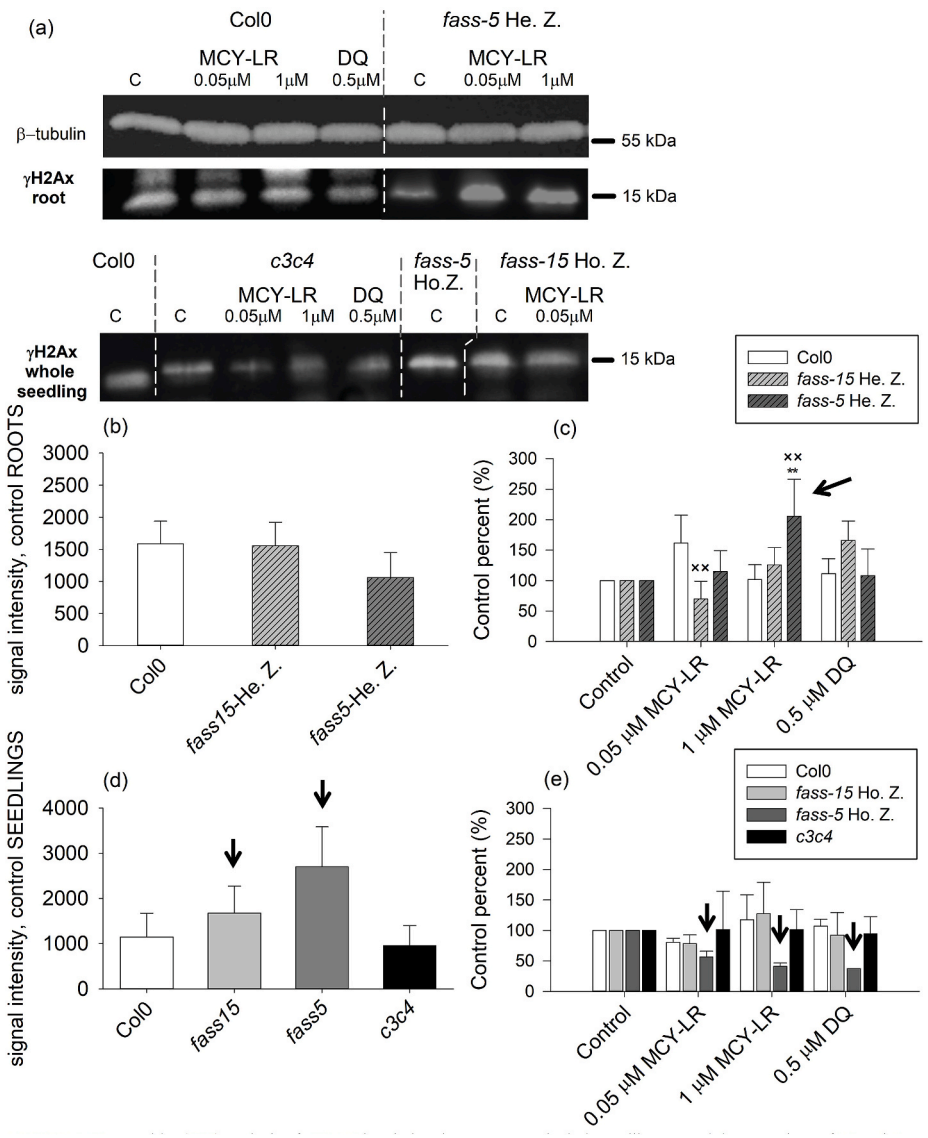

Fig. 3. Western blot (WB) analysis of γH2AX in whole primary roots and whole seedlings reveal that mutations of B" and C subunits as well as MCY-LR and DQ treatments alter its level. (**a**) Representative WB images for all genotypes, both controls and treatments. (**b, c**) Quantification of WB band intensities in roots for Col wt and *fass* heterozygotes, both controls and treatments. (**d, e**) Quantification of WB band intensities in whole seedlings of Col wt, *fass* homozygote recessives and *c3c4* (these mutant phenotypes are characterized by deformed very small or totally absent roots, as revealed in Materials and methods). Arrow on (c) shows increased levels of γH2AX in roots of *fass-5* heterozygotes in the presence of 1 μM MCY-LR. Arrows on (d) show increased levels of γH2AX in controls of *fass* mutants as compared to controls of Col0. Arrows in (e) show that both MCY-LR and DQ decreases γH2AX levels in *fass-5* homozygotes. Significant differences ($P < 0.05$) are indicated by ** (significance of differences between controls and treatments within a given genotype) and "XX" (significant differences as compared to Col0 controls) according to Section 2.5. of Materials and methods.

genotypes of *fass-5* and *fass-15* mutants for the B" regulatory subunit show higher levels of ROS, and 1 μM MCY-LR treatments induced their significant further increase (Fig. 1b, d). As we will see later, Cu/Zn-SOD activities do increase in *fass* mutants. What is the protein phosphatase background of these ROS levels? Mutants show that there is a partial difference between the involvement of B" and C subunits of PP2A in the regulation of ROS levels. In a study about to be published elsewhere, we demonstrated that protein phosphatase activities are not simply inhibited in *fass* and *c3c4*, rather the interaction between B" and C3/C4 subunits and the balance between PP2A and PP1 activities is altered differently in the two types of mutants. All of our results concerning ROS and γH2AX levels as well as SOD activities should be considered in the light of this statement as we will see below as well.

For *fass* homozygote controls, higher levels of ROS (mainly in root tips) are accompanied by higher activities of Fe1-SOD and Cu/Zn-SOD in whole seedlings (compare Fig. 1, arrows, to 4a). However, increased activities of these SOD isoforms are accompanied by decreased (and not increased, as for *fass*) ROS levels in controls of *c3c4* (Fig. 1d). Also, MCY-LR and DQ increase Cu/Zn-SOD activities in *fass*, but not in *c3c4* (compare Fig. 1b, d to 4d). This indicates that the lack of functional B vs C subunits affects differently SOD activities besides ROS levels, thus mutations and MCY-LR effects are influencing functionality and interaction of these subunits, rather than just decreasing PP2A activity. All these data indicate that both B" and C subunits of PP2A are involved in the regulation of ROS levels and scavenging (see also Fig. 6), although the possible complex interactions between these subunits at different subcellular localizations may explain that their roles/effects are only partially overlapping in this respect.

Transcription levels of the genes for different SOD isoforms are diverse in the presence of the same stress factor, like UV-B radiation (Kliebenstein et al., 1998). Concerning the activities of these isoenzymes, the present study shows that the control and MCY-LR/DQ-treated plants of different genotypes showed a different pattern in the changes of Fe1-SOD and Cu/Zn-SOD activities, when compared to Mn-SOD (where its activity remained relatively unchanged irrespectively to what genotype and what type of drug treatment did we use). For example, in case of controls, both Fe1-SOD and Cu/Zn-SOD activities were increased in whole seedlings of mutants as compared to Col0 (Fig. 4a). MCY-LR and DQ modulated Cu/Zn-SOD activities in Col0 as well as homo- and/or HeZs of *fass* (Figs. 4 and 5). Differences in the activities of isoforms are found in Cd treated Arabidopsis as well (Drążkiewicz et al., 2007). These are important findings that underline the differential responses of different SODs to changes of PP2A functionality and to abiotic stresses. Fe-SOD activity is known for being involved in oxidative stress defence. For example transgenic maize plants that overexpress Fe-SOD have increased tolerance to PQ (Van

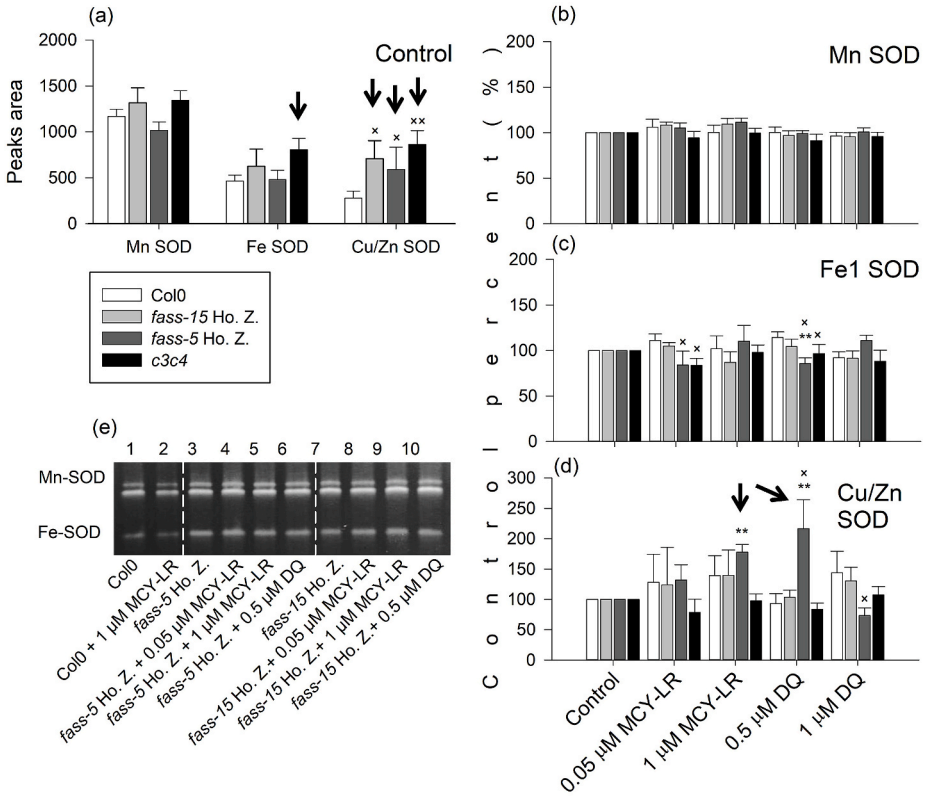

Fig. 4. Activity gels for SOD reveal that both B" and C subunits of PP2A modulate SOD activities and toxins increase their activities in a significant manner for Cu/Zn-SOD. Results for whole seedlings of Col wt and mutants (homozygote recessives for *fass*-5 and *fass*-15 as well as *c3c4*) are shown here. **(a)** Comparison of SOD activities of control seedlings of Col0, *fass-5*, *fass-15* and *c3c4*. **(b–d)** the effects of MCY-LR and DQ on the activities of (**b**) Mn-SOD; (**c**) Fe1-SOD; (**d**) Cu/Zn-SOD. Activities are expressed as raw data (a) and percentage of controls (100%) (b–d). Quantifications were performed as described in Materials and methods, Section 2.4. (**e**) A representative activity gel image for Mn-SOD and Fe-SOD. Significant differences ($P < 0.1$) are indicated by ** (significance of differences between controls and treatments within a given genotype) and "X" and "XX" (significant differences as compared to Col0 controls) according to Section 2.5. of Materials and methods.

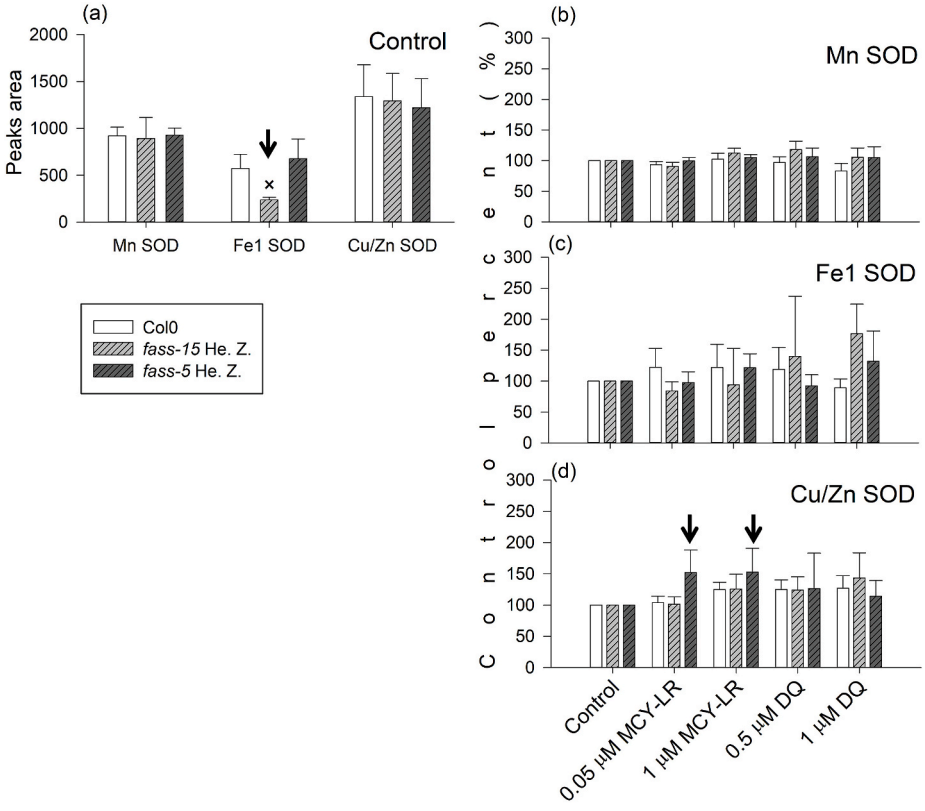

Fig. 5. Activity gels for SOD reveal that in primary roots, even the heterozygote genotypes of *fass* mutants show differences as compared to Col0 in the activities of Fe1-SOD, but not those of Mn-SOD and Cu/Zn-SOD **(a)**. Concerning the effects of MCY-LR and DQ, (**b**) Mn-SOD activities were not changed significantly. **(c)** Fe-SOD activities were increased by MCY-LR DQ in *fass-15*, although in a non-significant manner. (**d**) Cu/Zn-SOD activities were increased by DQ in *fass-15* and by MCY-LR in *fass-5* (see arrows for MCY-LR). Quantifications of activities were performed as for whole seedlings (see Fig. 4 and Materials and methods, Section 2.4.). Activities are expressed as raw data (a) and percentage of controls (100%) (b–d). Significant differences ($P < 0.1$) are indicated by "X" (significant differences as compared to Col0 controls).

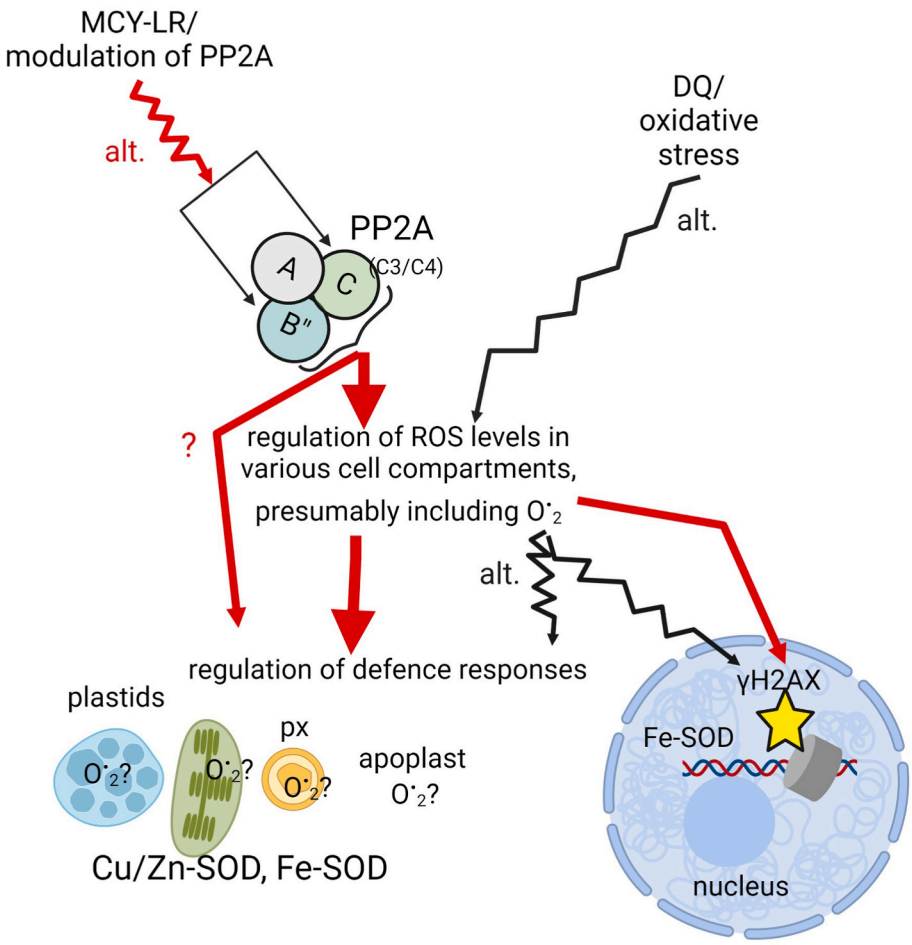

Fig. 6. Proposed model showing the involvement of B" and C3/C4 subunits of PP2A in the regulation of ROS and γH2AX levels and of SOD activities as well as the involvement of MCY-LR (protein phosphatase inhibitor) and DQ (ROS inducer) in these processes. Strong red arrows indicate the regulatory roles of B" and C subunits of PP2A. Irregular red arrows indicate the interference of MCY-LR with these processes via affecting B" and C subunits of PP2A, while black irregular arrows show the targets of DQ. Concerning SOD isoforms, this model proposes that the activities of Cu/Zn-SOD and to a less extent, Fe1-SOD, are regulated by these subunits of PP2A, and DQ affects them by a PP2A independent way. alt = alteration; px = peroxisomes. This Figure was created with BioRender.com.

Breusegem et al., 1999). In this study we show that Cu/Zn-SOD activities are the most sensitive to MCY-LR/DQ treatments in the *fass* mutants (Figs. 4d, 5d and 6). Cu/Zn-SOD activity is also modulated by different stress types. For example its activity is elevated during heavy metal stress by a mechanism involving ethylene (Abozeid et al., 2017). Trotta et al. (2011a, b) has already pointed out the role of the B'γ subunit of PP2A in modulating the activity/expression of this SOD isoform. Transgenic Arabidopsis plants that overexpress Mn-SOD are characterized by increased tolerance and the activity of other SODs, of catalase (CAT) and peroxidase (POD) is higher as well in these plants (Wang et al., 2004). All these data show that different SOD isoforms have different contributions to stress tolerance as dependent on the type of stress that the plants face.

All our data demonstrating alterations of SOD activities in PP2A/B" and C3/C4 mutants are among the first studies that show the involvement of these subunits in the regulation of ROS scavenging in plants. Fig. 6 will show a proposed model for this relationship.

4.2. B" and C3/C4 subunits of PP2A regulate H2AX phosphorylation in relation to ROS levels and scavenging

The phosphorylation of histone H2AX at a serine residue of the carboxy-terminus is mediated by members of the phosphatidylinositol 3-kinase family (ATM/ATR) in yeasts, mammals and plants (Fillingham et al., 2006; Roitinger et al., 2015). In mammals, PP2A plays a role in dephosphorylation of γH2AX, an event that is required for double-stranded DNA repair (Fillingham et al., 2006). What is the situation in plants? Phosphorylation of H2AX and intra-chromatin localization of γH2AX foci depends on multiple kinases (Moreno-Romero et al., 2012). However concerning serine-threonine phosphatases, PP2A controls the activity of ATM (Templeton and Moorhead, 2005), but knowledge is scarce regarding direct dephosphorylation of γH2AX by members of this phosphatase family. Here we demonstrate that (i) For controls of homozygote recessive *fass* mutants, increases of γH2AX levels (as compared to Col0) do show strong correlations with ROS levels, and there is a direct proportionality between these two parameters for controls of *c3c4* (compare Figs. 1 and 3d, decreases in both cases). These indicate that loss of B" subunit function induces both oxidative stress and DNA repair mechanisms, but this is not true for the C3 and C4 catalytic subunits: functions of PP2A B" and C3/C4 subunits are distinct in this respect, too. Since a loss of PP2A activities leads to the decrease and not the increase of H2AX phosphorylation state, we suggest that the C3 and C4 subunits of PP2A are not directly involved in γH2AX dephosphorylation; (ii) in case of *fass-5* homozygotes, there is an inverse proportionality between the increases of ROS levels and decreases of γH2AX levels in the presence of MCY-LR/DQ. Meanwhile, Western blot studies show that in *c3c4*, MCY-LR does not influence histone H2AX phosphorylation in a significant manner. One should note that MCY-LR treatments affect all five (thus, not only C3 and C4 that interact with FASS) subunits of PP2A, since it is a general PP2A inhibitor (Mackintosh and Diplexito, 2001). Overall, it seems that none of the C catalytic subunits are involved in direct dephosphorylation of γH2AX (compare Fig. 1b,d to Fig. 3e). Moreover, the increases of γH2AX levels in controls of *fass* mutants and decreases in *c3c4* as well the differences of MCY-LR effects between mutants and Col0 (Fig. 3) are also indicating that H2AX phosphorylation is regulated by the proper B"-C subunit interaction rather than by simply the dephosphorylation of γH2AX by PP2A. More clearly: if a subunit of PP2A is impaired in function, one would expect

hyperphosphorylation of putative substrates. According to our results we cannot suppose that any of the PP2A catalytic subunits have a direct role in γH2AX dephosphorylation in Arabidopsis. It should be noted that in the *fass* mutants, PP2A activity is not inhibited, rather an imbalance in PP2A-PP1 activities occurs and PP1 activity is higher than in controls (to be published elsewhere). Thus, we would expect a significant degree of γH2AX dephosphorylation in *fass*. However, γH2AX levels are increased in control *fass* mutants. We propose that the B" regulatory subunit plays a role in regulating H2AX phosphorylation via its proper interactions with catalytic subunits and not by directly modulating phosphatase activities.

What are the relationships of histone H2AX phosphorylation to ROS levels and scavenging? For controls, Fe1-SOD and Cu/Zn SOD activities are increased in the homozygote recessive *fass* and for *c3c4*. This occurs in a similar way to the increases of γH2AX levels and ROS levels in *fass* (compare Figs. 3a, 4a and 6). Thus it seems that oxidative stress responses co-occur with H2AX phosphorylation events in B" subunit mutants. However, MCY-LR/DQ treatments show decreases and not increases of γH2AX levels in *fass* and no change in *c3c4*, in contrast to the increase of Cu/Zn-SOD activities in *fass* and increases of ROS levels in all mutants. This suggests that H2AX phosphorylation is related to oxidative stress by a more complex way in Arabidopsis and this issue needs further investigation.

The *fass* mutants are showing a severely impaired developmental pattern only in case of the homozygote recessive phenotypes, while heterozygotes are seemingly normal (Kirik et al., 2012; Spinner et al., 2013). Therefore we expected that HeZs will show similar ROS levels, SOD activities and γH2AX levels to the wild type plants. To our surprise, at a comparison of heterozygotes and homozygote recessives to wild-type seedlings, this was not the case neither for controls, nor for MCY-LR/DQ treatments. Prominent discrepancies were for example (i) observed for γH2AX levels in controls (Fig. 3b, d); (ii) Fe1-SOD levels in controls (Figs. 4a and 5a); (iii) the effects of MCY-LR and DQ treatments on γH2AX levels in *fass* (compare Fig. 3c and e); and (iv) Fe1-SOD and Cu/Zn-SOD activities for both *fass-5* and *fass-15* (Figs. 4 and 5).

4.3. Final statements and conclusions

At a comparison of the effects of the two drugs, MCY-LR and DQ, we found only partial similarities concerning ROS levels and SOD activities (see Results section) to further demonstrate that MCY-LR may exert changes in the oxidative stress status of seedlings by its specific protein phosphatase inhibitory effect (see Fig. 6 as well). Concerning levels of γH2AX, the effects of the two toxins are only partially overlapping as well in Col0 plants: in tips of primary roots DQ, but not 1 μM MCY-LR increases γH2AX levels in a significant manner (Fig. 2c).

This paper is giving new insights into the regulation of ROS status in plant cells. Moreover, it may be a starting point for exciting future research to get a more comprehensive view of the PP2A-oxidative stress relationship in plants. For example, the "indirect phosphatase dependence" mentioned several times in this paper might involve that besides changes in SOD activities shown here, the expression levels of different SOD isoforms are altered in phosphatase mutants by diverse mechanisms. Overall, the main conclusions of the present work are:

(**i**) both C (catalytic C3 and C4) and B" (regulatory) subunits of PP2A are involved in the regulation of oxidative stress in Arabidopsis. B" subunit is prominent in the regulation of SOD activities (mainly Cu/Zn SOD and to a lesser extent, Fe1-SOD) involved in the oxidative stress defence responses. Relevant proofs: (**i/a**) both B" and C subunit mutants show different ROS levels as compared to Col0, concerning both control plants and the effects of MCY-LR/DQ treatments (Fig. 1). (**i/b**) in controls of *c3c4*, relatively low ROS levels show inverse proportionality to relatively high Fe1-SOD and Cu/Zn-SOD activities (compare Fig. 1b, d to Fig. 4a). This indicates that the C3 and C4 catalytic subunit isoforms of PP2A influence oxidative stress defence responses. (**i/c**) our results with the *fass-5* and *fass-15* mutants show that the FASS protein as a B" regulatory subunit does regulate oxidative stress and ROS scavenging, and it is related to histone H2AX phosphorylation. However, MCY-LR and DQ treatments show this relationship is complex, many aspects need further investigation. One should note that the functionality of the B" regulatory subunit has complex effects on PP2A activities (i.e. the lack of the functional protein does not mean that PP2A/C activity will be inhibited) and it affects other protein phosphatases (e.g. PP1) as well (to be published elsewhere). (**ii**) The involvement of B" subunit in the above processes depends not only on its presence or absence, but on its amounts/degree of activities as related to the PP2A holoenzyme-as revealed by comparisons in these terms of the homozygote recessive and heterozygote genotypes of *fass-5* and *fass-15* mutants. (**iii**) our findings have a toxicological aspect as well. Although many studies show that MCY-LR induces oxidative stress by mechanisms independent on its protein phosphatase inhibitory effects-we demonstrate that it is also inducing oxidative stress by modulating PP2A both in wild-type plants and B/C subunit mutants. Related to this, many of the effects of MCY-LR studied here are distinct to DQ, a ROS inducer with mechanisms of ROS induction at least partially independent of PP2A. (**iv**) Given the partially different effects of MCY-LR and DQ, the oxidative stress induction and responses are not totally dependent on PP2A in Arabidopsis. (**v**) the phosphorylation state of H2AX – which correlates to oxidative stress responses-seems not to be directly dependent on the modulations in the activity of the catalytic subunits of PP2A- but B" regulatory subunits do modulate γH2AX levels. Thus in Arabidopsis, PP2A activity given by the C3 and C4 (and other catalytic) subunits seems to play a minor direct role in γH2AX dephosphorylation as compared to other events related to B" subunits.

Our main findings are summarized in a model as shown on Fig. 6. This model shows how B" and C3/C4 subunits of PP2A are involved in oxidative stress responses and defence in Arabidopsis. The model also shows that MCY-LR and DQ act by different pathways: MCY-LR, as a PP2A inhibitor acts directly on the functionality of B" and C3/C4 subunits, thereby altering ROS homeostasis in Arabidopsis.

Author contributions

C.F. performed experimental design, most of the experiments, contributed to data analysis and made essential corrections to the manuscript. **T.G.** and **Z.K.** performed Western blots for γH2AX. **B. T-V.** contributed to activity gel electrophoresis for SOD. **M. M-H.** contributed to data analysis and manuscript corrections. **G.P.J.** and **A.K.** contributed to preparing protein extracts for biochemical analyses and immunohistochemistry of γH2AX as well as DCFDA labeling and analysis. **L. U–N.** performed confocal microscopy analysis of samples labeled immunohistochemically for γH2AX. **G.V.** purified MCY-LR. **C.M.** performed experimental design, contributed to DCFDA labelings, microscopy analyses and data analysis and wrote the manuscript.

Declaration of competing interest

The authors declare that they have no known competing financial interests or personal relationships that could have appeared to influence the work reported in this paper.

Data availability

Data will be made available on request.

Acknowledgements

This work was supported by the Hungarian research grants OTKA K120638 (CM) and K119647 (GV). C.F. was supported by the ÚNKP-22-4-I-DE-11 New National Excellence Program of the Ministry for Innovation and Technology from the source of the National Research, Development and Innovation Fund, Hungary as well as by the Scientia Amabilis Foundation. We would like to thank Dr. Martine Pastuglia (Institut Jean-Pierre Bourgin, INRA, Centre de Versailles) for kindly providing us with *fass* and *c3c4* seeds. We thank Mr. Peace Adedokun Oluwatosin for his help in performing Western blots, dr. György Vereb for the confocal microscopy facility and dr. Taras Pasternak for his advices in terms of whole mount immunohistochemical labeling.

References

Abozeid, A., Ying, Z., Lin, Y., Liu, J., Zhang, Z., Tang, Z., 2017. Ethylene improves root system development under cadmium stress by modulating superoxide anion concentration in *Arabidopsis thaliana*. Front. Plant Sci. 8, 253.

Acar, A., 2021. In vivo toxicological assessment of diquat dibromide: cytotoxic, genotoxic, and biochemical approach. Environ. Sci. Pollut. Res. 28, 47550–47561.

Apel, K., Hirt, H., 2004. Reactive oxygen species: metabolism, oxidative stress, and signal transduction. Annu. Rev. Plant Biol. 55, 373–399.

Ballesteros, I., Domínguez, T., Sauer, M., Paredes, P., Duprat, A., Rojo, E., et al., 2013. Specialized functions of the PP2A subfamily II catalytic subunits PP2A-C3 and PP2A-C4 in the distribution of auxin fluxes and development in Arabidopsis. Plant J. 73, 862–872.

Bertrand, R.L., Eze, M.O., 2014. Modifying polyacrylamide background color for the nitroblue tetrazolium-based superoxide dismutase staining assay. Adv. Enzym. Res. 77–81, 02.

Beyer, D., Tándor, I., Kónya, Z., Bátori, R., Roszik, J., Vereb, G., et al., 2012. Microcystin-LR, a protein phosphatase inhibitor, induces alterations in mitotic chromatin and microtubule organization leading to the formation of micronuclei in *Vicia faba*. Ann. Bot. 110, 797–808.

Bradford, M.M., 1976. A rapid and sensitive method for the quantitation of microgram quantities of protein utilizing the principle of protein-dye binding. Anal. Biochem. 72, 248–254.

Camilleri, C., Azimzadeh, J., Pastuglia, M., Bellini, C., Grandjean, O., Bouchez, D., 2002. The Arabidopsis TONNEAU2 gene encodes a putative novel protein phosphatase 2A regulatory subunit essential for the control of the cortical cytoskeleton. Plant Cell 14, 833–845.

Chen, J., Su, Y., Lin, R., Lin, F., Shang, P., Hussain, E., et al., 2021. Effects of acute diquat poisoning on liver mitochondrial apoptosis and autophagy in ducks. Front. Vet. Sci. 8, 727766.

Chen, H., Lee, J., Lee, J.M., Han, M., Emonet, A., Lee, J., et al., 2022. MSD2, an apoplastic Mn-SOD, contributes to root skotomorphogenic growth by modulating ROS distribution in Arabidopsis. Plant Sci. 317, 111192.

Creighton, M.T., Sanmartín, M., Kataya, A.R.A., Averkina, I.O., Heidari, B., Nemie-Feyissa, D., et al., 2017. Light regulation of nitrate reductase by catalytic subunits of protein phosphatase 2A. Planta 246, 701–710.

Drążkiewicz, M., Skórzyńska-Polit, E., Krupa, Z., 2007. The redox state and activity of superoxide dismutase classes in *Arabidopsis thaliana* under cadmium or copper stress. Chemosphere 67, 188–193.

Dvořák, P., Krasylenko, Y., Ovečka, M., Basheer, J., Zapletalová, V., Takáč, T., 2021. *In vivo* light-sheet microscopy resolves localization patterns of FSD1, a superoxide dismutase with function in root development and osmoprotection. Plant Cell Environ. 44, 68–87.

Farkas, I., Dombrádi, V., Miskei, M., Szabados, L., Koncz, C., 2007. Arabidopsis PPP family of serine/threonine phosphatases. Trends Plant Sci. 12, 169–176.

Fillingham, J., Keogh, M.C., Krogan, N.J., 2006. γH2AX and its role in DNS double-strand break repair. Biochem. Cell. Biol. 84, 559–568.

Freytag, C., Máthé, C., Rigó, G., Nodzyński, T., Kónya, Z., Erdődi, F., et al., 2021. Microcystin-LR, a cyanobacterial toxin affects root development by changing levels of PIN proteins and auxin response in Arabidopsis roots. Chemosphere 276, 1–10.

Fuchs, J., Demidov, D., Houben, A., Schubert, I., 2006. Chromosomal histone modification patterns – from conservation to diversity. Trends Plant Sci. 11, 199–208.

Gamborg, O.L., Miller, R.A., Ojima, K., 1968. Nutrient requirements of suspension cultures of soybean root cells. Exp. Cell Res. 50, 151–158.

Garda, T., Kónya, Z., Tándor, I., Beyer, D., Vasas, G., Erdődi, F., et al., 2016. Microcystin-LR induces mitotic spindle assembly disorders in *Vicia faba* by protein phosphatase inhibition and not reactive oxygen species induction. J. Plant Physiol. 199, 1–11.

Giannopolitis, C.N., Ries, S.K., 1977. Superoxide dismutases: I. Occurrence in higher plants. Plant Physiol. 59, 309–314.

Gill, S.S., Anjum, N.A., Gill, R., Yadav, S., Hasanuzzaman, N., Fujita, M., et al., 2015. Superoxide dismutase—mentor of abiotic stress tolerance in crop plants. Environ. Sci. Pollut. Res. 22, 10375–10394.

Jambunathan, N., 2010. Determination and detection of reactive oxygen species (ROS), lipid peroxidation, and electrolyte leakage in plants. In: Sunkar, E. (Ed.), Plant Stress Tolerance. 2010. Methods in Molecular Biology 639. Springer/Humana Press, NY-Dordrecht-Heidelberg-London, ISBN 978-1-60761-701-3, pp. 291–297.

Kataya, A.R., Heidari, B., Lillo, C., 2015. Protein phosphatase 2A regulatory subunits affecting plant innate immunity, energy metabolism, and flowering time – joint functions among B'η subfamily members. Plant Signal. Behav. 10, e1026024.

Kirik, A., Ehrhardt, D.W., Kirik, V., 2012. *TONNEAU2/FASS* regulates the geometry of microtubule nucleation and cortical array organization in interphase *Arabidopsis* cells. Plant Cell 24, 1158–1170.

Kliebenstein, D.J., Monde, R.A., Last, R.L., 1998. Superoxide dismutase in Arabidopsis: an eclectic enzyme family with disparate regulation and protein localization. Plant Physiol. 118, 637–650.

Konert, G., Trotta, A., Kouvonen, P., Rahikainen, M., Durian, G., Blokhina, O., et al., 2015. Protein phosphatase 2A (PP2A) regulatory subunit B′γ interacts with cytoplasmic ACONITASE 3 and modulates the abundance of AOX1A and AOX1D in *Arabidopsis thaliana*. New Phytol. 205, 1250–1263.

Kós, P., Gorzó, G., Surányi, G., Borbely, G., 1995. Simple and efficient method for isolation and measurement of cyanobacterial hepatotoxins by plant tests (*Sinapis alba* L.). Anal. Biochem. 225, 49–53.

Laemmli, U.K., 1970. Cleavage of structural proteins during assembly of the head of bacteriophage T4. Nature 227, 680–685.

Li, S., Mhamdi, A., Trotta, A., Kangasjärvi, S., Noctor, G., 2014. The protein phosphatase subunit PP2A-B′γ is required to suppress day length-dependent pathogenesis responses triggered by intracellular oxidative stress. New Phytol. 202, 145–160.

Liao, Y.D., Lin, K.H., Chen, C.C., Chiang, C.M., 2016. *Oryza sativa* protein phosphatase 1a (OsPP1a) involved in salt stress tolerance in transgenic rice. Mol. Breed. 36, 22.

Linkert, M., Rueden, C.T., Allan, C., Burel, J.-M., Moore, W., Patterson, A., et al., 2010. Metadata matters: access to image data in the real world. J. Cell Biol. 189, 777–782.

Ludwików, A., Cieśla, A., Kasprowicz-Maluśki, A., Mituła, F., Tajdel, M., Gałgański, Ł., et al., 2014. *Arabidopsis* protein phosphatase 2C ABI1 interacts with type I ACC synthases and is involved in the regulation of ozone-induced ethylene biosynthesis. Mol. Plant 7, 960–976.

Lv, Z., Zhao, M., Wang, W., Wang, Q., Huang, M., Li, C., et al., 2021. Changing Gyl311 to an acidic amino acid in the MATE family protein DTX enhances *Arabidopsis* resistance to the dihydropyridine herbicides. Mol. Plant 14, 2115–2125.

MacKintosh, C., MacKintosh, R.W., 1994. Inhibitors of protein kinases and phosphatases. Trends Biochem. Sci. 19, 444–448.

MacKintosh, C., Diplexcito, J., 2001. Chapter 102 - naturally occurring inhibitors of protein serine/threonine phosphatases. In: Bradshaw, R.A., Dennis, E.A. (Eds.), *Handbook Of Cell Signaling*. 2001. Academic Press, Burlington, ISBN 978-0-12-124546-7, pp. 607–611.

Máthé, C., Garda, T., Freytag, C., M-Hamvas, M., 2019. The role of serine-threonine protein phosphatase PP2A in plant oxidative stress signaling – facts and hypotheses. Int. J. Mol. Sci. 20, 3028.

Meinhard, M., Grill, E., 2001. Hydrogen peroxide is a regulator of ABI1, a protein phosphatase 2C from Arabidopsis. FEBS Lett. 508, 443–446.

Moreno-Romero, J., Armengot, L., Marquès-Bueno, M.M., Britt, A., Martínez, M.C., 2012. CK2-defective Arabidopsis plants exhibit enhanced double-strand break repair rates and reduced survival after exposure to ionizing radiation. Plant J. 71, 627–638.

Murashige, T., Skoog, F., 1962. A revised medium for rapid growth and bio assays with tobacco tissue cultures. Physiol. Plantarum 15, 473–497.

Nagy, M., Kéki, S., Rácz, D., Mathur, J., Vereb, G., Garda, T., et al., 2018. Novel fluorochromes label tonoplast in living plant cells and reveal changes in vacuolar organization after treatment with protein phosphatase inhibitors. Protoplasma 255, 829–839.

Pasternak, T., Tietz, O., Rapp, K., Begheldo, M., Nitschke, R., Ruperti, B., et al., 2015. Protocol: an improved and universal procedure for whole-mount immunolocalization in plants. Plant Methods 11, 50.

Roitinger, E., Hofer, M., Köcher, T., Pichler, P., Novatchkova, M., Yang, J., et al., 2015. Quantitative phosphoproteomics of the ataxia telangiectasia-mutated (ATM) and ataxia telangiectasia-mutated and rad3-related (ATR) dependent DNA damage response in *Arabidopsis thaliana*. Mol. Cell. Proteomics 14, 556–571.

Schindelin, J., Arganda-Carreras, I., Frise, E., Kaynig, V., Longair, M., Pietzsch, T., et al., 2012. Fiji: an open-source platform for biological-image analysis. Nat. Methods 9, 676–682.

Shi, Y., 2009. Serine/threonine phosphatases: mechanism through structure. Cell 139, 468–484.

Spinner, L., Gadeyne, A., Belcram, K., Goussot, M., Moison, M., Duroc, Y., et al., 2013. A protein phosphatase 2A complex spatially controls plant cell division. Nat. Commun. 4, 1863.

Tanaka, T., Halicka, D.T., Huang, X., Traganos, F., Darzynkiewicz, Z., 2006. Constitutive histone H2AX phosphorylation and ATM activation, the reporters of DNA damage by endogenous oxidants. Cell Cycle 5, 1940–1945.

Templeton, G.W., Moorhead, G.B.G., 2005. The phosphoinositide-3-OH-kinase-related kinases of *Arabidopsis thaliana*. EMBO Rep. 6, 723–728.

Trotta, A., Konert, G., Rahikainen, M., Aro, E.M., Kangasjärvi, S., 2011a. Knock-down of protein phosphatase 2A subunit B'γ promotes phosphorylation of CALRETICULIN 1 in Arabidopsis thaliana. Plant Signal. Behav. 6, 1665–1668.

Trotta, A., Wrzaczek, M., Scharte, J., Tikkanen, M., Konert, G., Rahikainen, M., et al., 2011b. Regulatory subunit B′γ of protein phosphatase 2A prevents unnecessary defense reactions under low light in Arabidopsis. Plant Physiol. 156, 1464–1480.

Van Breusegem, F., Slooten, L., Stassart, J.M., Moens, T., Botterman, J., Van Montagu, M., et al., 1999. Overproduction of *Arabidopsis thaliana* FeSOD confers oxidative stress tolerance to transgenic maize. Plant Cell Physiol. 40, 515–523.

Vasas, G., Gáspár, A., Páger, C., Surányi, G., Máthé, C., Hamvas, M.M., et al., 2004. Analysis of cyanobacterial toxins (anatoxin-a, cylindrospermopsin, microcystin-LR) by capillary electrophoresis. Electrophoresis 25, 108–115.

Waadt, R., Schmidt, L.K., Lohse, M., Hashimoto, K., Bock, R., Kudla, J., 2008. Multicolor bimolecular fluorescence complementation reveals simultaneous formation of alternative CBL/CIPK complexes in planta. Plant J. 56, 505–516.

Waadt, R., Manalansan, B., Rauniyar, N., Munemasa, S., Booker, M.A., Brandt, B., et al., 2015. Identification of Open Stomata-1 interacting proteins reveals interactions with sucrose non-fermenting1 related protein kinases 2 and with type 2A protein phosphatases that function in abscisic acid responses. Plant Physiol. 169, 760–779.

Wang, Y., Ying, Y., Chen, J., Wang, X., 2004. Transgenic *Arabidopsis* overexpressing Mn-SOD enhanced salt-tolerance. Plant Sci. 167, 671–677.

Yoon, J.T., Ahn, H.K., Pai, H.S., 2018. The subfamily II catalytic subunits of protein phosphatase 2A (PP2A) are involved in cortical microtubule organization. Planta 248, 1551–1567.

Zer, H., Chevion, M., Goldberg, I., 1993. Effect of paraquat on dark-grown *Phaseolus vulgaris* cells. Weed Sci. 41, 528–533.